Scientific Frontiers in Research on Extrasolar Planets
ASP Conference Series, Vol. 294, 2003
D. Deming and S. Seager, eds.

The Colors of Extrasolar Planets

Wesley A. Traub

Harvard-Smithsonian Center for Astrophysics, 60 Garden St., Cambridge MA 02138

Abstract. The color of an extrasolar planet is an important property because, for the case of direct detection, color is likely to be the first post-detection quantity to be measured. We show here that color carries considerable information on planetary properties. The next most likely measurable quantity is a low resolution spectrum, and we show what additional information this carries. Several other aspects of direct detection are discussed, including the respective benefits of visible and infrared detection, techniques of visible coronagraphic detection, and the spectroscopy of an Earth-like planet.

1. Introduction

The growing community of extrasolar planet astrophysicists is currently engaged in an active discussion of the respective merits of direct detection of extrasolar planets using visible (0.3 to 1.1 μm) vs. infrared (5 to 30 μm) techniques. Although much of this discussion centers on instrumentation considerations, there is a parallel dialog emerging that addresses the spectroscopic issue of how to extract planetary properties from a spectrum. These properties include diameter, mass, temperature, atmospheric composition, etc., and also the possible presence of life. In this paper we address a number of these issues, and focus at greater length on the visible spectrum as a rich source of planet properties.

2. Mass Distribution Function

A histogram of the masses of the 100 or so extrasolar planets that have already been detected shows a single-peak distribution centered between roughly 0.2 and 20 Jupiter masses. A log(mass) vs. number per interval in log(mass) space is the appropriate type of plot. The upper cutoff appears to be a real one, in the sense that there are very few companions to stars in the mass range from the deuterium-burning threshold (about 13 M_J) to the hydrogen-burning threshold (about 79 M_J). This is a region where the radial velocity searches are particularly sensitive, so the lack of detections suggests that there truly are few such objects.

The lower cutoff corresponds in magnitude and shape to a nominally expected limit imposed by the radial-velocity noise threshold range in the neighborhood from about 20 m/s for a highly significant detection, to about 2 m/s for a marginal detection. Doubtless future instrumental improvements will push the threshold somewhat lower, but probably not more than a factor of a few. The main point, however, is that the observed mass limit is consistent with a limitation of our instruments, not of the extrasolar planets themselves.

The only other data available are that of the solar system itself, which, if plotted on the same graph, show a nominally uniform distribution in number vs. log(mass) space, from about 1 M_J to 0.0001 M_J, actually rising slightly towards smaller masses. If we assume that the solar system is typical in this sense, then it follows that there are a large number of extrasolar planets waiting to be found, and in particular there may be at least as many terrestrial (Venus, Earth, Mars) planets as there are gas giants. This is a powerful reason to press forward with a search for extrasolar terrestrial planets.

3. Spectral Model

We have recently published a comprehensive first look at the spectral signature of an Earth-like planet, at visible and infrared wavelengths (Des Marais et al. 2002). The spectral model used for this analysis is outlined in Traub and Jucks (2002). The model includes all catalogued spectral lines in the range 0.3 to about 1000 μm wavelength, plus a number of as-yet-uncatalogued lines of which we are aware. In addition, band structures that have not as yet been resolved into individual lines are included. Reflectivity coefficients are also included for water, Rayleigh scattering, aerosol scattering, land-plant leaves, and phytoplankton.

The radiative transfer model permits thermal emission as well as reflectivity calculations. The model planet permits broken cloud layers as well as all of the above components. A simple box model is used to simulate the complex, and essentially unknowable, interactions of multiple scattering among the clouds, surface, and molecular atmosphere.

The calculations are detailed line-by-line, with sufficiently high spectral resolution to fairly represent the actual pressure-broadened and Doppler-broadened lines from the bottom to the top of the atmosphere (Traub & Stier 1976; Johnson et al. 1995). After calculating the high-resolution spectrum, a smearing function is applied to reduce the resolution to a value of about 100, which is convenient for the problem at hand.

The model atmosphere is that of the Earth, for an appropriate latitude and season. The integrated-Earth calculation is approximated by a single column at an appropriate slant angle which does a good job of approximating the full-Earth spectrum.

The model has been validated in three ways. First, this is the same model that we use to analyze our measured spectra of the Earth's stratosphere, taken with our Fourier transform spectrometer from a balloon-borne platform. Our analysis of spectra from about 15 balloon flights, and about as many aircraft flights, has shown that this model is highly reliable. Second, we have used this model to match the infrared observations of the Earth from a spacecraft enroute to Mars (Christensen & Pearl 1997), with good fidelity (Traub et al., in preparation). Third, we have used this model to match the measured visible spectrum of integrated Earth reflected light, as seen from the ground, in reflection off the dark side of the moon (Woolf et al. 2002).

4. Biomarkers in Visible and Infrared

Des Marais et al. (2002) conclude that the strongest biomarker (spectral evidence of life) on an extrasolar planet is a large abundance of molecular oxygen (O_2), followed by ozone (O_3), nitrous oxide (N_2O), methane (CH_4), and water (H_2O).

The reasoning for O_2 is that only life itself is believed capable of producing large amounts of oxygen, although from several examples in the solar system it is possible to produce small amounts of oxygen by purely photochemical means. Oxygen can only be seen in the visible.

Ozone is interesting because it is a highly nonlinear indicator of the presence of oxygen, in the sense that a small amount of oxygen can produce a relatively large amount of ozone; large amounts of oxygen can produce larger amounts of ozone, but the relationship remains nonlinear. Thus, ozone could be used as an early indicator of oxygen, but it saturates quickly, and is not useful as an indicator of larger amounts of oxygen. Ozone can be seen in the infrared as well as the visible.

Nitrous oxide is produced only by life, and so is a good indicator of life. However, the only useful N_2O band is in the infrared at about the same position as methane and water, so will be difficult (at best) to interpret in a faint signal.

Methane is produced by life, but it is also a primordial gas, so is ambiguous. Methane can be seen in the infrared and in the near-infrared.

Water is essential for life, in forms that we understand. Water vapor is easily detectable in many wavelength regions, and its presence in significant amounts will be both a sign that the extrasolar planet is in the habitable zone (where surface water is in liquid form), and that there is free water on the surface of the planet.

Two other spectral signatures are valuable as biomarkers, total molecular gas column, and the "red edge" of land-plant leaves (sometimes known as the chlorophyll signature). Neither of these is mentioned in the Des Marais et al. report, because there we only considered molecular absorption features. Nevertheless, these are valuable spectral markers.

Total gas can be recognized by its Rayleigh scattering signal, a very strong ultraviolet component. The importance of total gas column is that it is an indicator that we are seeing to an identifiable pressure level. Since Rayleigh scattering is essentially independent of molecular species, it is an excellent indicator of total gas column.

Land plant leaves have a small reflectivity at green wavelengths, making them look green of course, but a relatively very large reflectivity at red wavelengths, from about 0.72 μm to at least about 1.0 μm wavelength. This "red edge" pattern is not duplicated by any other substance of which we are aware, and is therefore a good marker for the presence of land plants.

5. Visible Wavelength Coronagraph

The visible reflected flux from the Earth, near maximum elongation, is about 10^{-10} times fainter than the sun, and at a nominal distance of 10 pc, the Earth-sun separation is about 0.1 arcsec. No existing coronagraph can operate in this parameter range. However in the past year or so, two classes of coronagraph designs have been proposed, either of which is theoretically capable of resolving such a system, and allowing us to record a planet spectrum with little interference from its parent star. We classify these designs as pupil-plane or image-plane coronagraphs. In all cases the goal is to reduce the intensity of light that is diffracted outside the core image by as much as 8 orders of magnitude, so that the diffracted intensity is less than the planet intensity. The advantages of this approach are discussed by Kuchner and Spergel (2003).

Pupil-plane coronagraphs have a mask in the pupil plane, so the mask can be at the primary mirror itself, or downstream at an image of the primary mirror. One type is a family of graded-transmission masks such as proposed by Nisenson and Papaliolios (2001), and another type is the family of binary-transmission masks such as discussed in Kasdin, Spergel, and Littman (2002). All of these designs apodise the shape or intensity profile of the incident wavefront, so that, for example, it acquires a gaussian profile in at least one dimension, and therefore the image, a Fourier transform of the incident wavefront, also has a gaussian shape, and therefore has steeply-falling wings.

Image-plane coronagraphs have a mask in the image plane. Here too there is a family of graded-transmission masks such as proposed by Kuchner and Traub (2002), and a family of binary-transmission masks proposed by Kuchner and Spergel (2002). These designs diffract an on-axis point-source image such that downstream at a re-imaged pupil plane there are multiple copies of the original pupil with phases and amplitudes arranged such that essentially complete cancellation occurs over a large part of the re-imaged pupil. A Lyot mask in this plane blocks any remaining non-canceled starlight, usually in a narrow ring around the edge of the pupil. A final image plane then contains a zero or very weakened star image, plus nearly the full intensity of any off-axis source such as a planet.

6. Infrared Wavelength Interferometer

The infrared emitted flux from an Earth is about 10^{-6} times that of a sun in the 10 μm region. An interferometer can be arranged such that the various collected segments of wavefront are phase and amplitude adjusted such that when they combine they will produce a nearly zero output for an on-axis point source. These are known as nulling interferometers. (From the point of view of the wavefront, the net result is similar to that of a nulling image-plane coronagraph, as discussed above.)

Several nulling interferometer designs have been proposed. One is the "TPF booklet" design (Beichman et al. 1999), and another is the Darwin design (Fridlund 2000, 2003). These both comprise several free-flying infrared telescopes to collect the light, relay optics to feed the light to a central station, phase-flipping and amplitude scaling optics on some of the beams, and a combiner to put the summed beams onto a detector. These designs are discussed at some length in the references, so will not be further discussed here. Woolf (2003) argues the case for an infrared interferometer for extrasolar planet detection.

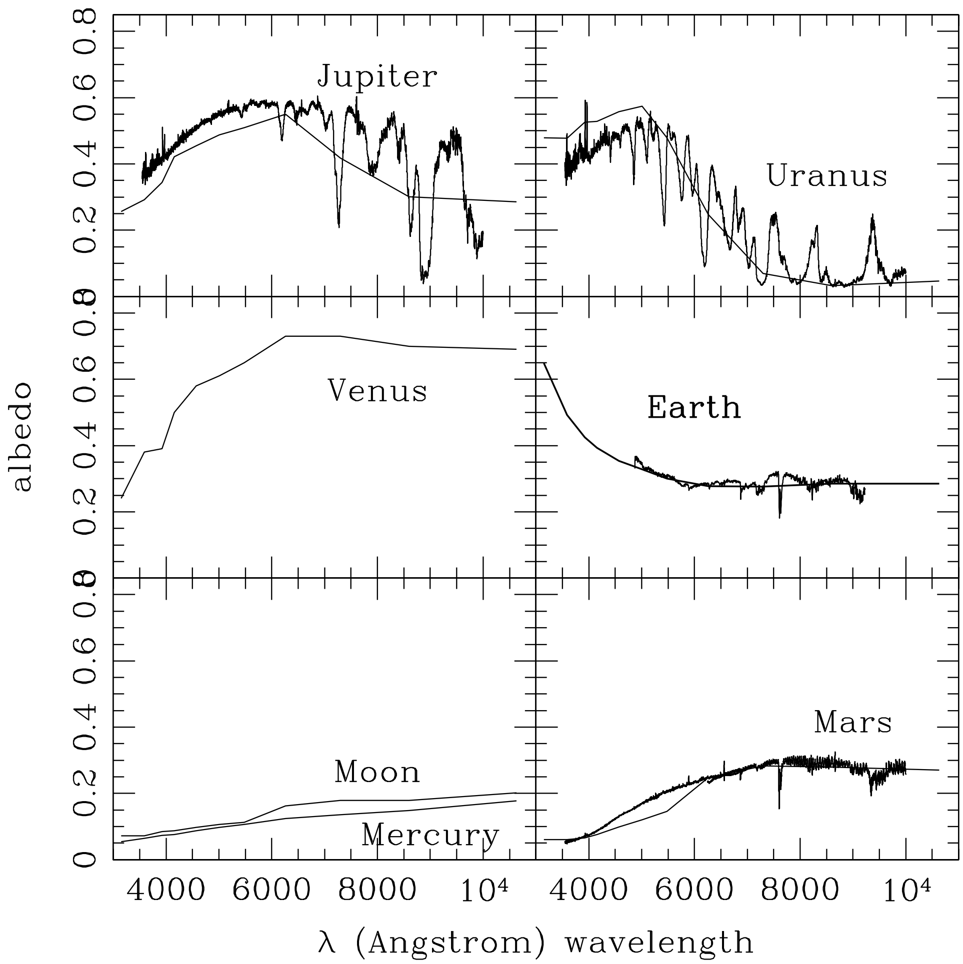

Figure 1. Filter photometry (which implies color) and low-resolution spectra for seven solar system objects are shown for the visible spectral range. The rocky objects have rather smooth, red spectra (the Mars spectrum has some incompletely-removed terrestrial features). The gas giants have depressed red albedoes. Cloud-covered Venus has a depressed blue albedo. The Earth has an enhanced blue albedo, from Rayleigh scattering, plus its oxygen and water features. From these basic types we may infer underlying properties.

7. Color Implies Properties

Visible Wavelengths. The visible wavelength color of a planet can be used to infer many properties, as we shall briefly argue here, and at greater length elsewhere (in preparation). In Figure 1 we show filter photometer data for seven solar system objects, with medium-resolution spectra superposed as an aid to interpreting the data. The filter data are mostly from Irvine et al. (1968), and the spectra are from our own unpublished observations. It is obvious from these photometric curves, and the low-resolution components of the spectra, that the general curve shape in each of the 6 boxes is different from the others. For example, if you partition each spectrum into, say, 1000-angstrom chunks, you could still distinguish each of these curves.

Suppose that we can use curves of this type to distinguish rocky planets from gas giants, i.e., only two basic groups. Suppose also that any other type of planet that we might envision via theoretical calculations can be similarly classified. We note that the flux from a planet depends on the albedo and radius, and the mass depends on the radius and mean density. It follows that the mass can be expressed as a function of density, flux, and albedo, and that the radius is a function of flux and albedo.

From data on the solar system objects, we find that the gas giants and rocky planets have variances of density and albedo, which when combined with an assumed flux uncertainty of 10%, say, allows us to estimate the mass and radius. The result is that for a rocky planet we can expect to estimate the mass to about 44% and the radius to 14%. For a gas giant the uncertainties are 50% in mass and 14% in radius. These results are totally empirical, and apply strictly only to the solar system. Nevertheless these relations give a nominal idea of what inferences we might draw regarding an extrasolar planet.

Temperature can also be estimated, using the fact that equilibrium temperature is a function of albedo and radius (given that the star flux is well understood). The result is that temperature can be estimated to about 3% for rocky planets, and 5% for gas giants.

Atmospheric pressure can be estimated as well. We start by using the blue Rayleigh scattering signal to estimate the column abundance to an accuracy of 20%, say. Then we use the derived radius and mean density to calculate surface gravity. Combining these values we derive the atmospheric pressure at the base of the visible gas column, with a total accuracy of about 27% for a rocky planet.

Infrared Wavelengths. Planet properties can also be estimated from infrared photometry and spectroscopy. In the clear portions of the infrared spectrum, between major absorption bands of CO_2, O_3, and H_2O for example, the measured continuum flux can be used to infer a temperature. Then the flux and temperature will imply an area, giving the planet radius. Then if the spectrum can be used to infer if the planet is terrestrial or gas giant in nature, the mass can be estimated.

However despite this relatively direct connection between infrared spectrum and radius, there are some parameters that cannot be estimated from the infrared. In particular, there is no known estimator of pressure (analogous to Rayleigh scattering), oxygen cannot be measured in the infrared, and the chlorophyll "red edge" has no infrared counterpart.

8. Conclusion

We see that many interesting extrasolar planet properties can be estimated from measurements of the colors and low-resolution spectra in the visible. In particular, the biomarkers oxygen, ozone, and chlorophyll are found in the visible, and planetary properties such as temperature, pressure, radius, and mass can be estimated from visible colors and spectrum.

References

Beichman, C. C., Woolf, N. J., & Lindensmith, C. A. 1999, eds., JPL publication 99-3; also at http://tpf.jpl.nasa.gov

Christensen, P. R. & Pearl, J. C. 1997, JGR, 102, 10875

Des Marais, D. J., Harwit, M., Jucks, K. W., Kasting, J. F., Lunine, J. I., Lin, D., Seager, S., Schneider, J., Traub, W. A., & Woolf, N. 2002, Astrobiology 2002, 2, 153

Fridlund, M. 2000, ed., ESA publication ESA-SCI(2000), 12

Fridlund, M. 2003, these proceedings

Irvine, W. H., Simon, T., Menzel, D. H., Pikoos, C., & Young, A. T. 1968, AJ, 73, 807

Johnson, D. G., Jucks, K. W., Traub, W. A., & Chance, K. V. 1995, JGR, 100, 3091

Kasdin, N. J., Spergel, D. N., & Littman, M. G. 2002, submitted to Appl.Opt.

Kuchner, M. J., & Spergel, D. N. 2002, submitted to ApJ

Kuchner, M. J., & Spergel, D. N. 2003, these proceedings

Kuchner, M. J., & Traub, W. A. 2002, ApJ, 570, 900

Nisenson, P., & Papaliolios, C. 2001, ApJ, 548, L201

Schneider, J. 2002, http://cfa-www.harvard.edu/planets

Traub, W. A. & Jucks, K. W. 2002, in Atmospheres in the Solar System, Comparative Aeronomy, ed. M. Mendillo, A. Nagy, & J. H. Waite (Wash. DC, AGU), 369 (astro-ph/0205369)

Traub, W. A., & Stier, M. T. 1976, Appl. Opt., 15, 364

Woolf, N. J., Smith, P. S., Traub, W. A., & Jucks, K. W. 2002, ApJ, 574, 430 (astro-ph/0203465)

Woolf, N. J. 2003, these proceedings

Wes Traub